Energy Vol. 13, No. 6, pp. 529–536, 1988
Printed in Great Britain.

0360-5442/88 $3.00 + 0.00

A HEAT–POWER CYCLE FOR ELECTRICITY GENERATION FROM HOT WATER WITH NON-AZEOTROPIC MIXTURES

CHU-JUN GU[1] and LAN LIN[2]

[1]Thermal Energy Research Institute, Tianjin University, Tianjin and [2]Department of Power Engineering, Beijing Graduate School, North-China Institute of Electric Power, Qinghe, Beijing, China

(*Received* 18 *June* 1987; *received for publication* 19 *January* 1988)

Abstract—A new heat–power cycle is introduced. This cycle is suitable for electricity generation using relatively low temperatures for hot water or other fluids. The cycle provides improved electricity generation over the Carnot and the Lorenz cycles. We suggest a practical plan for applying the new cycle to electricity generation at moderate temperatures.

INTRODUCTION

The binary fluid cycle system for electricity generation using relatively low-temperature heat is currently used widely. The traditional binary fluid cycle system is the Rankine cycle system with a single working fluid of low-boiling point. The Carnot cycle is an approximation of the Rankine cycle. Figure 1 shows the Carnot cycle a–b–c–d–a for hot-water power generation. In Fig. 1, hot-water releases heat with its temperature raised by the heat source at temperature T_f to T_e. The cooling water absorbs heat while its temperature is changed from T_h to T_g.

In a power-generation system, there is an optimal evaporation temperature for which the power output per unit mass of hot water is a maximum. With a minimum temperature difference δT_e for heat exchange in the evaporator, we have

$$T_e = T_a + \delta T_e. \tag{1}$$

Thus, T_e is determined by T_a and

$$T_a \approx (T_h T_f)^{1/2}. \tag{2}$$

Generally, T_e is larger than T_h. Therefore, hot water with temperature T_e is not used to produce power but drained. If we consider only the limitation of the minimum temperature difference for heat exchange, the areas a–m–b–a and d–c–n–d in Fig. 1 are not used to produce power. Therefore, the efficiency of the Carnot cycle system is lower than that of the cycle which possesses the area n–a–m–c.

In 1984, a Lorenz power cycle with a working fluid consisting of a non-aezotropic mixture for power generation was suggested. Figure 2 shows the Lorenz cycle a–b–c–d–a. In the Lorenz cycle, the evaporation process a–b of a non-aezotropic mixture is not isothermal but rather has a variable temperature between T_a and T_b. Similarly, the condensation process has a variable temperature between T_c and T_d. For the Lorenz cycle, line a–b in Fig. 2 is parallel to line d–c.

Although the Lorenz cycle is similar to the Carnot cycle, it is not a perfect cycle. There is an optimal evaporation temperature

$$T_a \approx -T_f + [2T_f(T_f + T_h)]^{1/2}. \tag{3}$$

Therefore, the hot water with temperature T_e is not used to produce power but drained; T_c is generally larger than T_h. Because of the claim that line a–b is parallel to line d–c in the Lorenz cycle, area h–g–g′–h(=limit of the area h–g–g″–h) in Fig. 2 is not used to produce power.

The following is an important question: can we find a new power cycle which possesses perfect performance for power generation for the given hot-water source temperature, the specified inlet temperature of cooling water and the given minimum temperature difference for heat exchange?

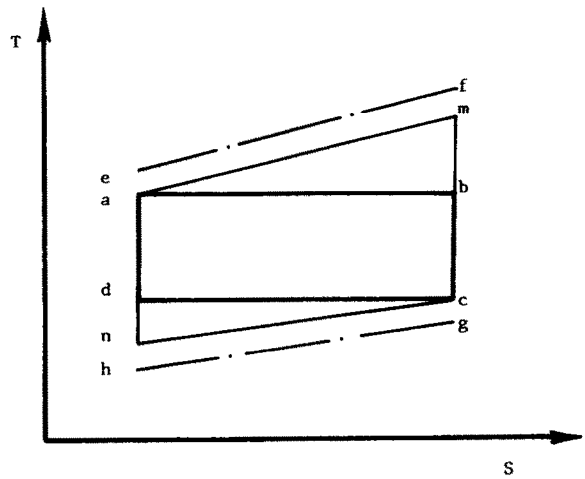

Fig. 1. The Carnot cycle in the T–S plane.

In 1986, Chu-Jun Gu suggested that a new heat–power cycle[2] yields improved performance for power generation, as compared with the Carnot and Lorenz cycles under the same operating conditions. This cycle will now be described.

A NEW HEAT-POWER CYCLE

The new cycle is shown in Fig. 3. In the new cycle a–b–c–d–a, the line a–b represents the evaporation process with temperature increasing from T_a to T_b; line c–d corresponds to condensation with the temperature decreasing from T_c to T_d; line b–c represents isentropic expansion; and line d–a corresponds to isentropic compression.

Figure 4 shows a comparison of the Carnot and Lorenz cycles with the new cycle. For the given hot-water source temperature, the given inlet temperature for water condensation, and the given minimum temperature difference for heat exchange (which is determined by the optimal evaporation temperature), the work for the Carnot cycle is represented by area a′–b′–c–d′–a′ in Fig. 4, while the work for the Lorenz cycle is represented by the area a″–b–c″–d″–a″. The work for the new cycle is represented by the area a–b–c–d–a. It is apparent that the power output per unit mass of hot-water for the new cycle is much greater than for either the Carnot or the Lorenz cycle.

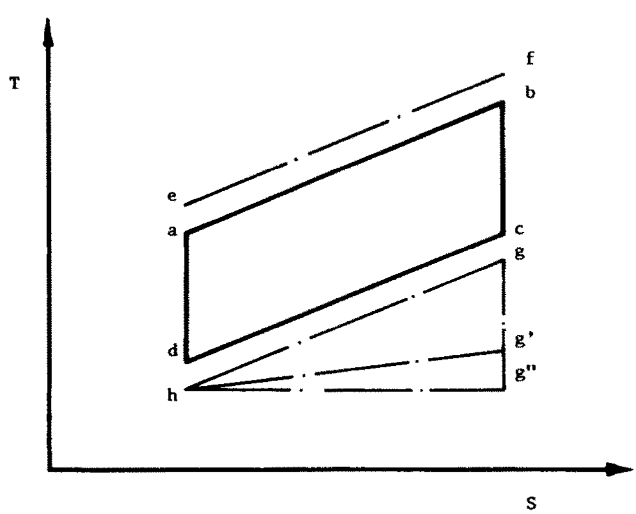

Fig. 2. The Lorenz cycle in the T–S plane.

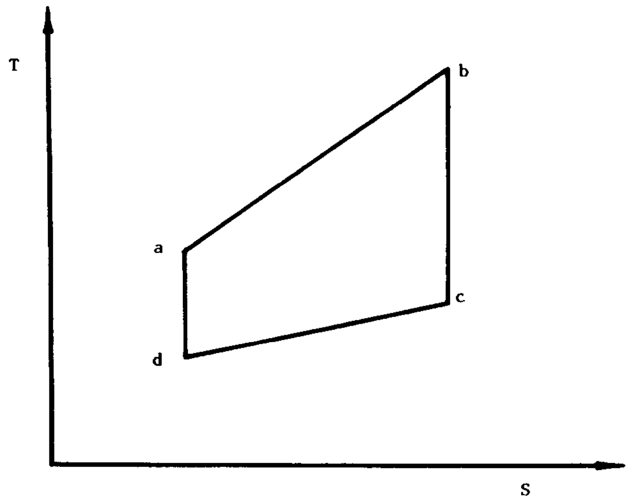

Fig. 3. The new cycle in the T–S plane.

When the temperature differences for heat exchange are the same everywhere in the heat exchanger, this heat exchanger has been matched optimally and the resulting heat exchange is defined to be the optimal heat exchange. The irreversibly lost work is a minimum in the optimally matched heat exchanger. In the new cycle, both an optimally matched evaporator and condenser are used.

Figure 5 shows a new multistage cycle a_n–b_1–c_1–d_1–c_2–d_2– . . . c_n–d_n–a_n, where line a_n–b_1 represents an evaporation process with temperature changing from T_{an} to T_{b1}, line b_1–c_1 represents an isentropic expansion process and line d_n–a_n corresponds to an isentropic compression process. The condensation process includes multistage condensation processes c_1–d_1, c_2–d_2, . . . , c_n–d_n. The work of the new multistage cycle is represented by area a_n–b_1–c_1–d_1–c_2–d_2 . . . c_n–d_n–a_n, and this area is equal to the area a_n–b_1–c_1–d_n–a_n, which is the area of one stage in the new cycle a_n–b_1–c_1–d_n–a_n. It can be proved that

$$\begin{aligned} W_n &= \text{area}\quad a_n\text{–}b_1\text{–}c_0\text{–}d_n\text{–}a_n - \text{area}\quad c_1\text{–}c_0\text{–}d_1\text{–}c_1 - \text{area}\quad c_2\text{–}d_1\text{–}d_2\text{–}c_2 \ldots \\ &\quad - \text{area}\quad c_n\text{–}d_{n-1} - d_n - c_n \\ &= \text{area}\quad a_n\text{–}b_1\text{–}c_0\text{–}d_n\text{–}a_n - \tfrac{1}{2}\text{area}\quad a_0\text{–}c_1\text{–}c_0\text{–}d_n\text{–}a_0 \\ &= \text{area}\quad a_n\text{–}b_1\text{–}c_1\text{–}d_n\text{–}a_n = W_1 \\ &= \tfrac{1}{2}(S_{b1} - S_{an})(T_{an} - T_{dn} + T_{b1} - T_{c1}), \end{aligned} \tag{4}$$

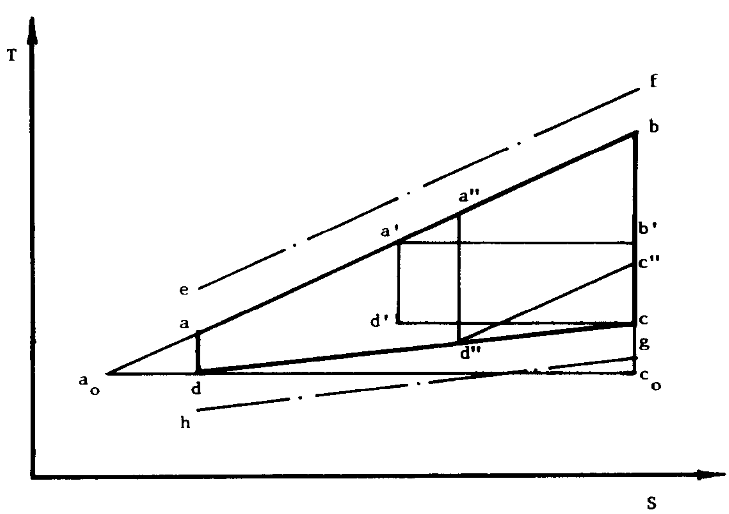

Fig. 4. Comparison of the new cycle with the Carnot and Lorenz cycles.

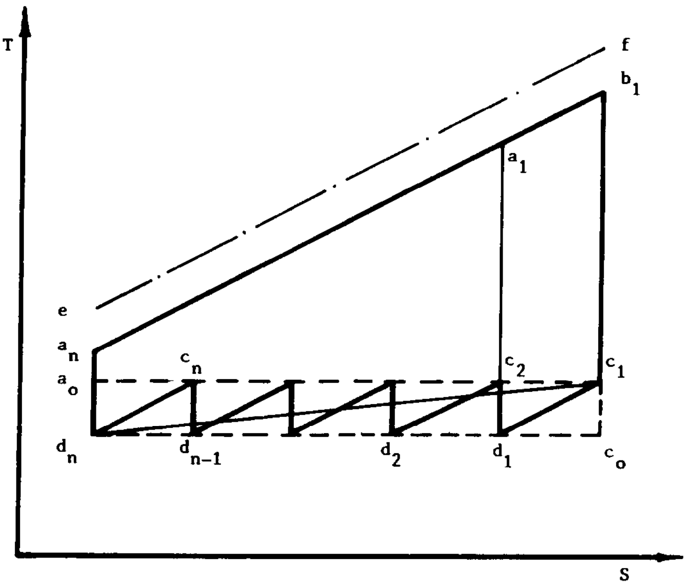

Fig. 5. The new multistage cycle in the T–S plane.

where W_n is the work for n stages of the new cycle a_n–b_1–c_1–d_1–c_2–d_2 . . . c_n–d_n–a_n, W_1 is the work for one stage of the new cycle a_n–b_1–c_1–d_n–a_n; S_{b1}, S_{an} are entropies at the points b_1 and a_n in the cycle, respectively. T_{an}, T_{dn}, T_{b1}, T_{c1} are the temperatures of the points a_n, d_n, b_1, and c_1 in the cycle, respectively.

Therefore, W_n is determined only by the characteristic points b_1, c_1, d_n, a_n of the new cycle and has no relation to the number of stages used. This is an important character of the new cycle, which simplifies computations. For this reason, only one stage of the new cycle is analysed in this paper (cf. Figs. 3 and 4). The heat released per unit mass of hot-water is

$$Q_h = C_pA(T_f - T_e), \tag{5}$$

where C_p is the (assumed constant) specific heat of water and A is the unit-conversion coefficient. The flow rate of the working fluid in the binary fluid-cycle system is

$$G = 2Q_h/[(S_b - S_a)(T_a + T_b)]. \tag{6}$$

The power output per unit mass of hot-water is

$$\begin{aligned} W_g &= AC_p(T_f - T_e)(S_b - S_a)(T_a - T_c + T_b - T_d)/[(S_b - S_a)(T_a + T_b)] \\ &= AC_p(T_b - T_a)(T_a - T_c + T_b - T_d)/(T_a + T_b) \\ &= AC_pT_b(1 - \lambda_b - \lambda_c + \lambda_a\lambda_c + \lambda_a\lambda_b - \lambda_a^2)/(1 + \lambda_a), \end{aligned} \tag{7}$$

where $\lambda_a = T_a/T_b$ represents the extent to which hot-water energy is utilized and is called the energy-utilization coefficient; $\lambda_b = T_c/T_b$ represents the temperature change of the working fluid during condensation and is called the temperature-variance coefficient for condensation; $\lambda_c = T_d/T_b$ represents the temperature change of the cooling water and is called the temperature coefficient of the cooling water.

The derivative of W_g with respect to λ_a is

$$\partial W_g/\partial\lambda_a = AC_pT_b\{2[(\lambda_b - \lambda_a) - (\lambda_a - \lambda_c)] - (1 - \lambda_a)^2\}/(1 + \lambda_a)^2. \tag{8}$$

If $T_a > T_c$, then $\lambda_a > \lambda_b > \lambda_c$, $\partial W_g/\partial\lambda_a < 0$, and the output of the new cycle increases as the temperature T_a decreases. For $\partial W_g/\partial\lambda_a = 0$,

$$\lambda_a = \lambda_a^0 = [2(\lambda_c + \lambda_b)]^{1/2} - 1; \tag{9}$$

and the corresponding temperature is

$$T_a^0 = [2T_b(T_c + T_d)]^{1/2} - T_b; \tag{10}$$

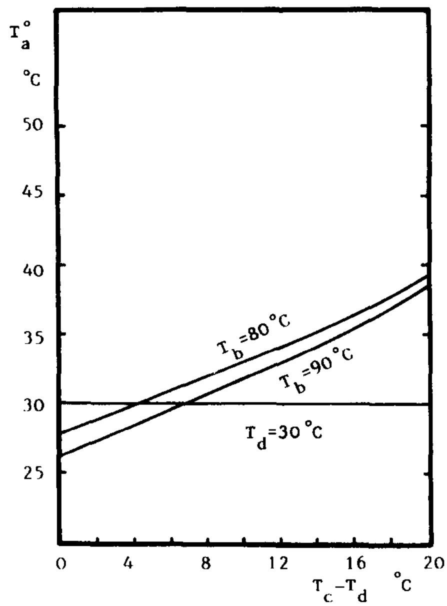

Fig. 6. The temperature T_a^0 as a function of temperature difference $T_c - T_d$.

when $T_a < T_a^0$,

$$\partial W_g / \partial \lambda_a > 0. \tag{11}$$

Equation (11) indicates that the power output of the new cycle decreases as T_a decreases for $T_a < T_a^0$. The power output W_g is maximized when $T_a = T_a^0$ and this maximum power output decrease as T_a^0 increases. Furthermore, T_a^0 increases as T_c increases and, therefore, $T_c - T_d$ must be as small as possible for maximal power output. Figure 6 shows the temperature T_a^0 as a function of the temperature difference $T_c - T_d$.

The first derivative of W_g with respect to λ_b is

$$\partial W_g / \partial \lambda_b = A C_p T_b (\lambda_b - 1)/(\lambda_a + 1) < 0. \tag{12}$$

Equation (12) indicates that the power output always increases as T_c decreases. For an optimally-matching condenser, the very small temperture difference $T_c - T_d$ will make the flow rate of cooling water so large that the required heat exchange in the condenser is difficult to obtain.

From Figs. 4 and 6, we can see that the temperature T_a is close to T_d when the condensation-temperature drop is sufficiently small, i.e., $T_c - T_d < 10°$ C. Thus, the new cycle approximates the cycle a_0–b–c_0–a_0 in Fig. 4. Therefore, the power output of the new cycle is larger than that for all other possible cycles, for given temperatures of the hot-water source, and cooling water and a minimum temperature difference for the heat exchanger. This conclusion is also correct for power-generation systems using sensible heat sources of working fluids other than water.

A METHOD FOR REALIZING THE NEW CYCLE

Under the conditions of given pressure and mixture composition, non-azeotropic binary mixtures of miscible refrigerants condense and boil over a temperature range. Since the temperature variance between the boiling and dew points is not large, it is difficult to utilize the new cycle by using only a one-stage cycle. We now present a method which can be used to realize the new heat–power cycle by using a multistage cycle. The new multistage cycle is shown on the T–S diagram of Fig. 7. The equipment arrangement that may be used is shown in Fig. 8.

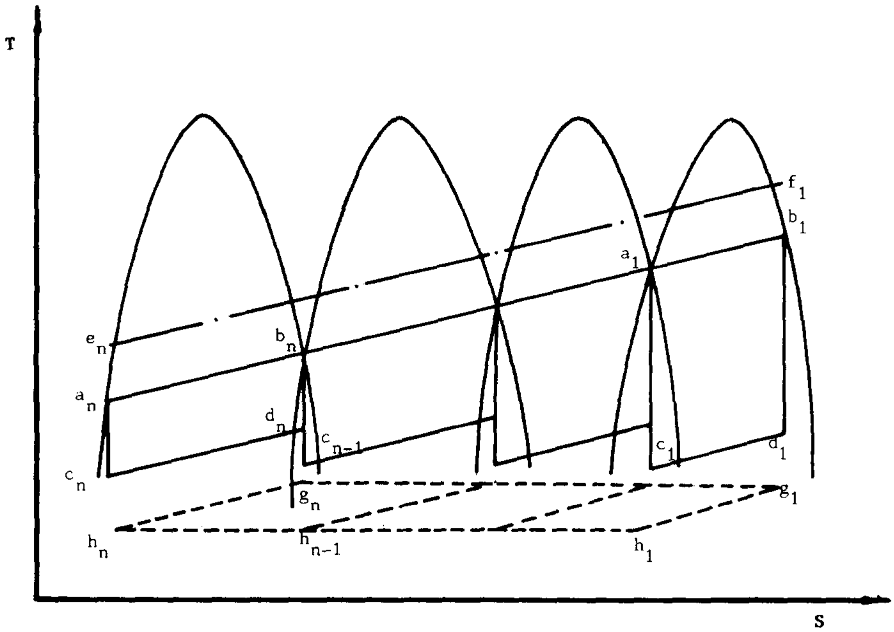

Fig. 7. The T–S diagram for the new multistage cycle.

The method suggests that hot-water flows through several evaporators successively (the number of evaporators is equal to n) with the temperature varying from T_{f1} to T_{en}. Non-azeotropic mixtures are turned into vapor in n sets of evaporators. The vapors of the mixtures, which enter n sets of turbines, ideally expand at constant entropy from b_1 to d_1, b_2 to $d_2, \ldots, b_n$ to d_n, respectively, to produce power, and the processes of condensation from d_1 to c_1, d_2 to $c_2, \ldots, d_n$ to c_n occur when cooling waters enter n sets of condensers, respectively, to carry away the rejected heat. The condensates are returned to the entrances of n sets of evaporators by n sets of pumps, and the new multistage cycle repeats.

We have now concluded the thermodynamic calculation for the new multistage cycle with non-azeotropic binary mixtures R12/R142b. The evaporators and condensers have been matched optimally in the calculation.

The parameters chosen for the calculation are: (i) the temperature of hot-water source = $T_{f1} = 90°C$; (ii) the hot-water flow rate = $G_e = 50T/h$; (iii) the temperature of the cooling water = $T_{h1} = 20°C$; (iv) the temperature difference for heat exchange in the evaporators = $\delta T_e = 10°C$; (v) the temperature difference for heat exchange in the condensers = $\delta T_c = 10°C$; (vi) the molar concentrations of mixtures are divided into four groups = $X_{R12} = 0.5$, 0.6, 0.7, 0.8. The results for the new multistage cycle, the Lorenz cycle and the Carnot cycle are shown in Table 1. The number of stages for the new multistage cycle is equal to 12.

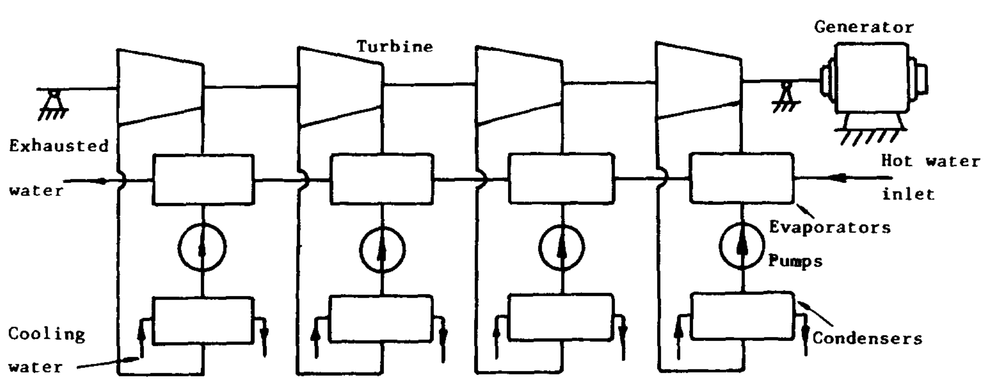

Fig. 8. The schematic of the new multistage cycle equipment.

Table 1. Comparison of power output for the Carnot cycle, the Lorenz cycle and the new multistage cycle.

Types of cycles	Working fluids	Power output per unit mass of hot water and increasing rate of power output	Units	Concentration (X_{R12})			
				0.5	0.6	0.7	0.8
Carnot cycle	R12	Power output per unit mass of hot water	kJ/T	7063.897	6824.908	6715.024	6804.589
Carnot cycle	R142b	Power output per unit mass of hot water	kJ/T	7066.998	6828.289	6718.728	6808.037
Lorenz cycle	R12/R142b	Power output per unit mass of hot water	kJ/T	7970.689	7939.993	7911.953	7893.882
	—	Increase of power output compared with the Carnot cycle R12	%	12.84	16.34	17.82	15.95
		Increase of power output compared with the Carnot cycle R142b	%	12.78	16.28	17.76	16.01
The new cycle	R12/R142b	Power output per unit mass of hot water	kJ/T	14653.339	14401.599	14270.853	14383.094
	—	Increase of power output compared with the Lorenz cycle	%	83.62	81.38	80.37	82.21
		Increase of power output compared with the Carnot cycle R12	%	107.18	111.02	112.52	111.37
		Increase of power output compared with the Carnot cycle R142b	%	107.09	110.91	112.40	111.27

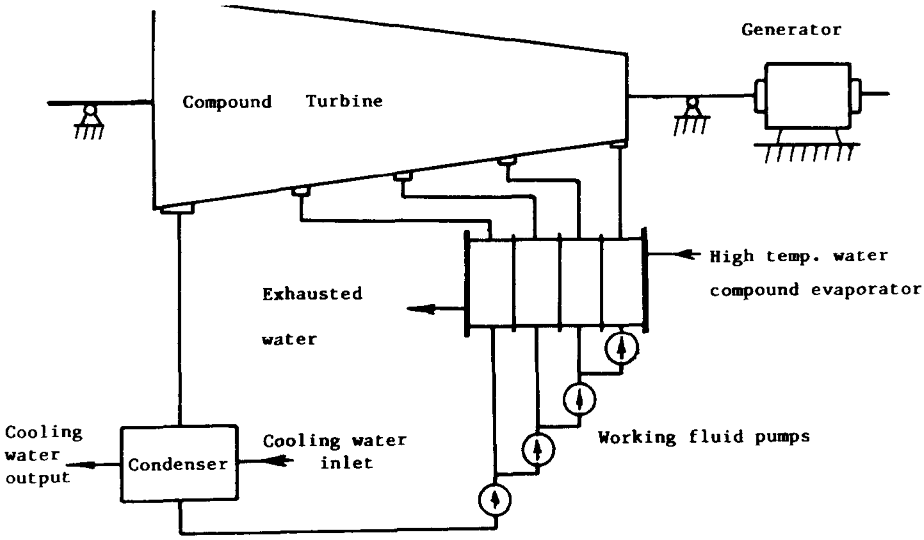

Fig. 9. The schematic of the new compound cycle equipment.

In the new multistage heat-power cycle, a compound turbine with n vapor inlets and a compound evaporator can be used to reduce the cost and the size of the new multistage cycle equipment. The equipment arrangement in the new compound cycle is shown in Fig. 9.

CONCLUSION

In the binary fluid-cycle system for hot-water electricity generation, the power output per unit mass of hot-water obtained from the new cycle is greater than for the Carnot and Lorenz cycles.

For the given hot-water source temperature difference, given inlet temperature for condensation water, and given minimum temperature difference for the heat exchanger, the new heat-power cycle is the optimal, technically feasible heat-power cycle.

In the new heat-power cycle with non-azeotropic mixtures, the condensation temperature drop $T_c - T_d$ (cf. Fig. 4) should be as small as possible in order to produce the maximal power output. The new multistage cycle can be constructed with compound power generation system that is economic and technically feasible.

REFERENCES

1. Chih Wu, *Int. J. Energy Systems* **4,** 21 (1984).
2. Chu-Jun Gu, "Exergy Analysis of a New Heat Power Cycle," in "The Third Symposium on Energy Savings of the Chinese Society for Engineering Thermophysics," Beijing (June 1986).
3. Chu-Jun Gu and Lan Lin, "Exergy Analysis on a Reverse-Flow Heat Exchanger Using Refrigerant Mixtures," in Ref. 2.
4. Chu-Jun Gu, "Study of a New Heat Power Cycle," Conference on Engineering Thermophysics of the Chinese Society for Engineering Thermophysics, Wenzhou, China (November 1986).
5. Chu-Jun Gu, Yi-Tai Ma, and Canren Lu, "Simulated Computation and Experimental Study of a Heat Pump Using Refrigerant Mixtures R12/R142b," *J. Engng. Thermophys., China* **8,** 10 (1987).
6. Zhimai He, Yufeng Zhang, and Chu-Jun Gu, "The Evaluation and Analysis of Heat Pump Cycles for Non-Azeotropic Mixtures," *J. Engng. Thermophys., China* **8,** 20 (1987).